

Experimental study of flame propagating behaviors through titanium particle clouds

Wei Gao^{*†}, Toshio Mogi^{*}, Xiaobo Shen^{**}, Jianzhong Rong^{***},
Jinhua Sun^{**}, and Ritsu Dobashi^{*}

^{*}Department of Chemical System Engineering, School of Engineering, The University of Tokyo, Hongo7-3-1, Bunkyo-ku, Tokyo 113-8656, JAPAN

Phone: +81-3-5841-1799

[†]Corresponding address: gaowei@chemsys.t.u-tokyo.ac.jp

^{**}State Key Laboratory of Fire Science, University of Science and Technology of China, Hefei, Anhui 230027, PR CHINA

^{***}Sichuan Fire Research Institute of Ministry of Public Security, Chengdu, Sichuan 610036, PR CHINA

Received: February 11, 2013 Accepted: July 18, 2013

Abstract

To determine the flame propagation mechanisms in titanium dust explosions, titanium particles at two concentrations were dispersed by air into a one end closed chamber to form dust clouds, and the mixtures were ignited by an electric spark. A high-speed video camera was used to record the flame propagation process and to obtain direct light-emission photographs. The flame temperature was detected by a fine thermocouple comprising 25- μm -diameter Pt-Pt/Rh13% wires. Based on the experimental results, the oxidation, combustion state and combustion mechanism of the titanium particles were analyzed. The propagation velocity and temperature characteristics of the combustion zone were also elucidated in detail. It was found that after ignition, the flames began to propagate quickly and emitted strong white light in the vertical chamber and the combustion state of the titanium particles strongly depended on the titanium concentration. Additionally, the flame propagation was faster and the temperature increased earlier and reached a higher value at a dust concentration of $1000\text{ g}\cdot\text{m}^{-3}$ than at $500\text{ g}\cdot\text{m}^{-3}$.

Keywords : titanium particle cloud ; flame propagation behavior ; flame temperature

1. Introduction

Explosion behavior of metals is of practical interest because of the frequency of accidental dust explosions during the manufacturing, processing, and handling of combustible particulate metals. The industrial distribution of dust explosions in China and Japan, as shown in Figure 1, indicates that metal dust explosions account for a large proportion of dust explosions. In addition to maximizing safety, a good understanding of the basic combustion mechanisms involved in these explosions is important for sensitizing the explosives used in mining, and similar considerations play a role in the mechanism of this sensitization. Of the metal elements, titanium is usually included in igniters and pyrotechnic formulations because of its ignitability and complete burnout, which enables the

full use of its high heat of reaction. In contrast to aluminum and boron, the explosion characteristics of titanium are not fully understood, especially regarding the flame propagation characteristics in dust explosions, which must be known to prevent accidents and minimize the damage in case of an accident.

Shafirovich¹⁾ studied the combustion of a single titanium particle using electrodynamic balance (levitation) and laser ignition. The results indicated that oxygen diffusion in the gas phase played a major role in the combustion mechanism of $100\mu\text{m}$ or larger titanium particles in air, while the chemical kinetics was more important for smaller particles. Kelzenberg²⁾ observed the burning behavior of titanium powder as a bulk material on a 1 g scale in oxygen flow inside a window bomb. Kelzenberg

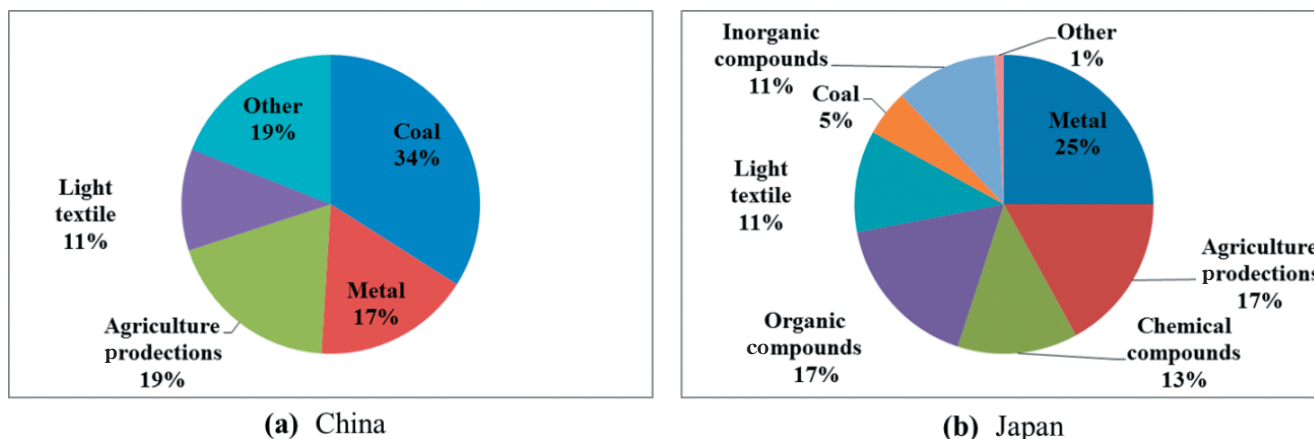


Figure 1 Industry distribution of dust explosions in China and Japan

reported that the combustion of titanium as a bulk material was a complex process that was governed not only by the evaporation of fuel and the diffusion of oxygen to the surface and into the titanium matrix but also by the oxidation reaction of the titanium melt, which seemed to be best described as an exothermic solution of O atoms in titanium, and the precise physico-chemical properties of melting, evaporation, and decomposition of different titanium oxides. Molodetsky³⁾ revealed the phases of titanium combustion in air, showing that the maximum combustion temperature was considerably less than the boiling temperatures of both titanium and its oxides. A particle radiation brightness jump was observed during the combustion in addition to particle explosion, which terminated burning. Hertzberg⁴⁾ and Kenneth⁵⁾ measured the explosion limit, pressure, and temperature of titanium particles in a standard 20L explosion test chamber. Previous studies of flame propagation have primarily focused on the characteristics of organic particles, such as monobasic alcohols⁶⁾, starch^{7),8)}, lycopodium^{9),10)}, and stearic acid^{11),12)}. Based on the studies mentioned above, there is an obvious lack of research on the flame propagation characteristics of titanium particles in dust explosions.

In this study, to reveal the flame propagation mechanisms of titanium particles in dust explosions, experiments have been conducted in a one end closed chamber. The propagation processes and temperature characteristics of the combustion zone, flame structure, and combustion process of titanium particles are determined at two titanium concentrations.

2. Experimental apparatus

Most of the sensitivity and severity parameters of dust explosions were measured in the dust explosion chambers specified by the internationally accepted ASTM standards, such as the Hartmann tube, and the 20L spherical explosion test chamber. These apparatuses were suitable for measuring the minimum ignition energy, minimum explosible concentration, maximum explosion pressure and deflagration index¹³⁾ but were inconvenient for examining the flame structure and flame propagation mechanisms.

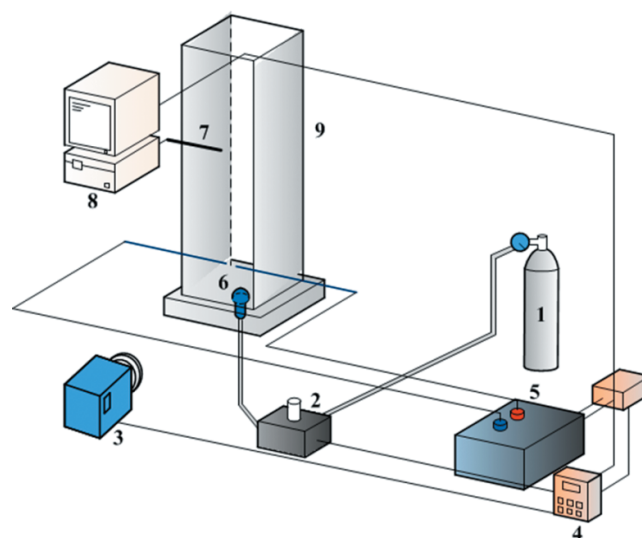


Figure 2 Experimental apparatus:
 1. Gas tank,
 2. Electromagnetic valve,
 3. High speed camera,
 4. Time controller,
 5. High voltage transformer,
 6. Ignition electrodes,
 7. Thermocouple,
 8. Data recorder,
 9. Chamber

In this study, an experimental system similar to the traditional Hartmann tube was designed to observe the flame propagation of particles in dust explosions. The experimental apparatus is schematically shown in Figure 2 and was composed of a small-scale combustion chamber, a gas-supplying unit, an ignition system, a thermocouple, a data recorder system, a high-speed video camera, and a time controller system. The small-scale combustion chamber was 500 mm in height with a square cross-section of 80 mm×80 mm. The top end was open and the bottom end was closed. To conveniently observe the flame propagation process, two sides of the chamber wall were constructed using a glass material, and two sides were constructed using stainless steel. A gas nozzle, a dispersing cone, and a sample plate were mounted at the bottom of the chamber. The ignition system consisted of a high-voltage transformer and a pair of tungsten wire electrodes with a 0.4 mm diameter positioned 50 mm above

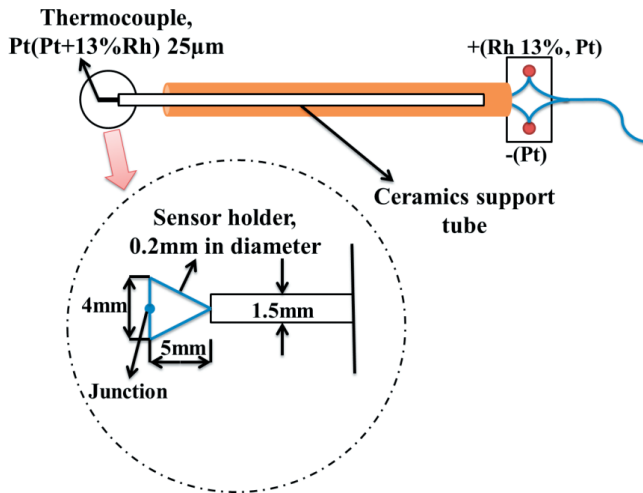


Figure 3 Structure of the thermocouple

the bottom of the chamber. The distance between the tips of the two electrodes was approximately 5 mm. A high-voltage transformer with an output of 30 kV was used to create the ignition spark. The ignition duration was 0.01 s and the nominal ignition energy was approximately 30 J.

The temperature measurement system consisted of a thermocouple and a data recorder. The thermocouple was comprised of 25 µm-diameter Pt-Pt/Rh13% wires. The structure of the thermocouple is shown in Figure 3.

In the experiments, the startup times of the high-speed video camera, the data recorder, the high-voltage igniter, and the on-off time of the electromagnetic valve were controlled using an Omron synchronization controller. The detailed experimental conditions are as follows: ignition voltage, 30 kV; discharge period, 0.01 s; framing rate of high-speed video camera, 2000 frames·s⁻¹; injection time, 0.5 s; pressure in the tank, 0.4 MPa.

2.3 Material

Titanium has a low density and is a strong, lustrous, corrosion-resistant (including resistance to sea water, aqua regia, and chlorine) and transition metal with a silver color. Like aluminum and magnesium metal surfaces, titanium metal surfaces oxidize immediately when exposed to air. The titanium powder used in this study was provided by the Nilaco Corporation of Japan. The particle size and purity are 44 µm and 99.3%, respectively. The physical and chemical properties of the titanium particles are presented in Table 1⁴.

Thermo-gravimetric analysis (TGA) was conducted to obtain detailed information regarding the thermal weight. Figure 4 shows the weight changes that occurred upon heating. To ensure that the atmosphere was the same as that in the experiments, air was used as the atmosphere for the TGA analysis. The heating rate was 10K·min⁻¹. The weight of the titanium began to increase at approximately 600°C, and when the temperature reached 980°C, the oxidation reaction almost completely stopped. The weight increase ratio of the titanium particles was approximately 165.74%.

Some SEM pictures of the titanium particles are shown in Figure 5, indicating an irregular structure with sharp

Table 1 Physical-chemical characteristics of titanium.

Name	Titanium
Formula	Ti
Phase	Solid
Molecular weight [kg/kmol]	47.867
Density [g/cm ³]	4.506
Melting Point [K]	1941
Boiling Point [K]	3560
Heat of fusion [kJ/mol]	14.15
Heat of vaporization [kJ/mol]	425
Molar heat capacity [J/mol K]	25.060
Thermal conductivity ¹ [W/mK]	0.1529
Thermal diffusivity ¹ [mm ² /s]	0.1755
Specific heat ¹ [mJ/mm ³ K]	0.8740

¹Thermal conductivity, thermal diffusivity and specific heat were measured by Hot Disk TPS2500s Thermal Properties Analyzer.

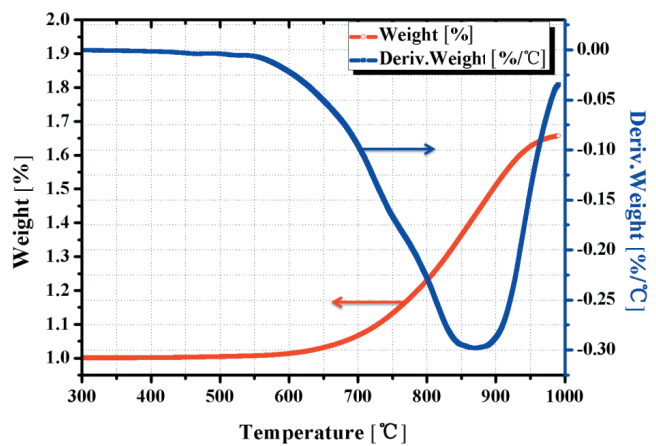


Figure 4 TGA profile of Titanium particles

edges. The larger particle surface areas promote the reaction with air.

The actual particle size distributions were measured using a laser diffraction analyzer and are shown in Figure 6. The Sauter diameter $D_{[3,2]}$, the volume diameter $D_{[4,3]}$, and the specific surface area are 21.209 µm, 25.960 µm, and 0.283 m²·g⁻¹, respectively.

3. Experimental results and discussion

3.1 Oxidation and combustion state of titanium particles

Many researchers have found that the oxidation of titanium corresponds not to simple molecular reactions but to an exothermic process of continuously solving oxygen in the solid or liquid titanium matrix¹⁵. Classically denoted condensed titanium oxides, such as TiO, Ti₂O₃, Ti₃O₅, and TiO₂, only provide the mixture ratio. In the solid phase, some of these formulas can be correlated to crystal structures. In the gaseous phase, only TiO and TiO₂ are identified as molecules¹⁶.

The oxidation of titanium is a highly exothermic process, as shown by the following reaction equations for various titanium oxides.

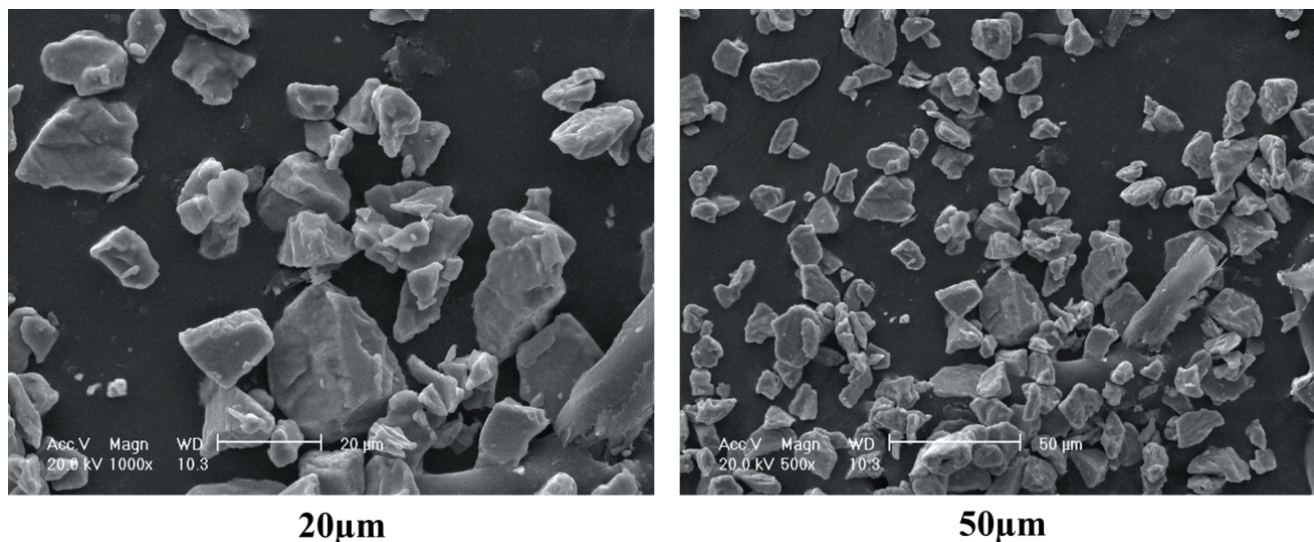


Figure 5 SEM photographs of Titanium particles

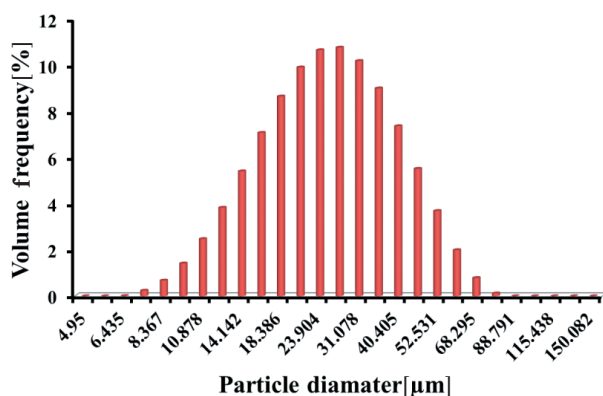
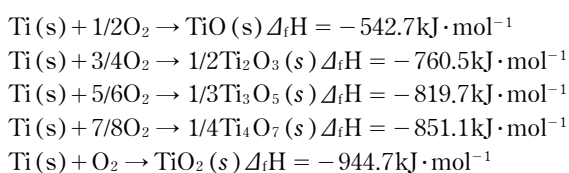


Figure 6 Diameter distribution of Titanium particles



Another important issue in analyzing titanium particle combustion is whether the reactions occur on the solid/liquid surface (heterogeneous combustion) or in the gas phase (homogeneous combustion). The combustion reaction state of the titanium particle is determined not only by the heat of combustion but also by its specific heat, the heat of fusion, and the latent heat of vaporization. To estimate the combustion reaction state of the titanium particle, Hertzberga⁴⁾ defined the fraction of the dust particle that can vaporize within the flame front as:

$$\beta = 26.3 \frac{p_{eg} [\text{bar}]}{d_p [\text{cm}] \rho [\text{g} \cdot \text{m}^{-3}]} \left[\frac{M [\text{g} \cdot \text{mol}^{-1}]}{T [\text{K}]} \right]^{1/2} \quad (1)$$

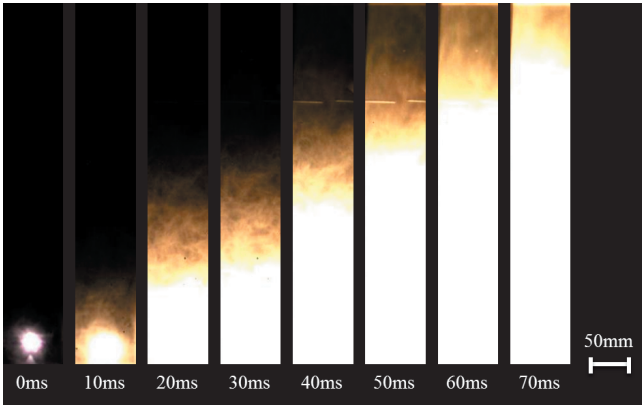
Where p_{eg} is the equilibrium vapor pressure at temperature T , d_p is the particle diameter, ρ is the particle density, and M is the molecular weight of its vapor species. If the calculated β value at $T_{ad,max}$ for a titanium particle exceeds unity, a homogeneous mechanism for titanium particle is supported; however, β at $T_{ad,limit}$ is

essentially zero, which suggests that a heterogeneous surface phase oxidation mechanism may be the only realistic mechanism. This finding indicates that the combustion state of titanium particles strongly depends on the concentration of the dust cloud.

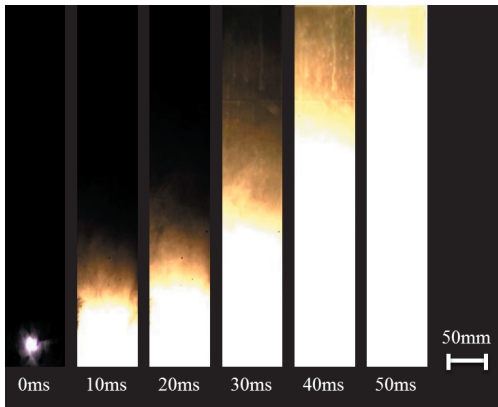
3.2 Flame propagation behavior

The calculated stoichiometric concentration, C_{st} , for reaction with air was $419 \text{g} \cdot \text{m}^{-3}$. Hertzberga⁴⁾ measured the minimum explosible concentration of titanium particles in the standard 20 L explosion chamber under two igniters: $80 \text{g} \cdot \text{m}^{-3}$ for a 2,500J igniter and $65 \text{g} \cdot \text{m}^{-3}$ for a 5,000J igniter. In this study, the flame propagation processes in the titanium dust clouds at two titanium concentrations ($500 \text{g} \cdot \text{m}^{-3}$ and $1000 \text{g} \cdot \text{m}^{-3}$) were recorded by a high-speed video camera. Before ignition, two methods were combined to determine the initial concentration and distribution of the particles. Two hardboards were inserted into the chamber just after dispersion to capture the particles. After two minutes, the two hardboards were weighed on an electrobalance to determine the mass of the particles in different sections¹⁷⁾. In addition, a laser sheet was used to illuminate the flow field and a high speed camera with Nikon 200mm Micro lens was used to observe the distributions of the particles. Combining the above two methods, it was proved that the distribution of particles was quasi-uniform.

Figure 7 shows a series of typical high-speed video stills recorded by the high-speed video camera with a normal lens, revealing the flame propagation processes through the titanium dust clouds in the vertical chamber. As shown in Figure 7, after the titanium particle cloud was ignited by the electrical spark, the flames began to propagate in the chamber. In the initial stage, the flames propagated in all directions, and the downward flames propagated more quickly than those in other directions. After approximately 8.5ms and 4.5ms for the lower and higher concentrations, respectively, the downward flames reached the bottom of the chamber. The flames reached the chamber walls 11.5ms and 6.5ms after ignition for the



(a). $500 \text{ g}\cdot\text{m}^{-3}$



(b). $1000 \text{ g}\cdot\text{m}^{-3}$

Figure 7 High-speed direct photographs of flame propagation process at two concentrations; frame rate: $2000 \text{ frames}\cdot\text{s}^{-1}$; time from ignition.

lower and higher concentrations, respectively, after these developments only upward propagation continued. In the upward propagation process, the flames propagated quickly and emitted a strong white light. The length of the luminous zone increased during flame propagation, and a thin yellow light zone gradually appeared in front of the white light zone.

According to the experimental results described above and the chemical and physical properties of titanium and

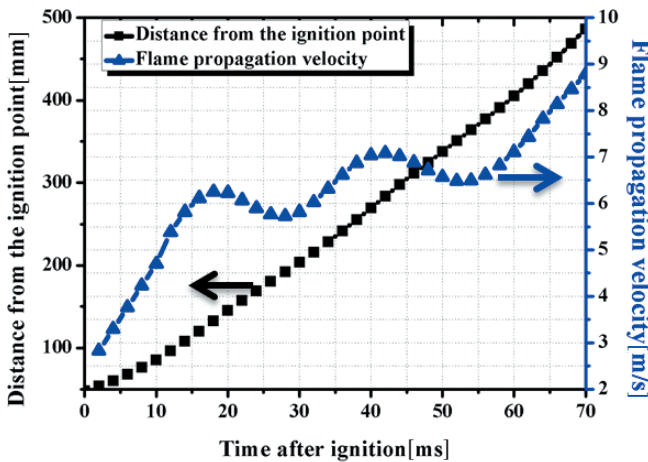


Figure 8 Microexplosion process of the burning titanium particle²⁾.

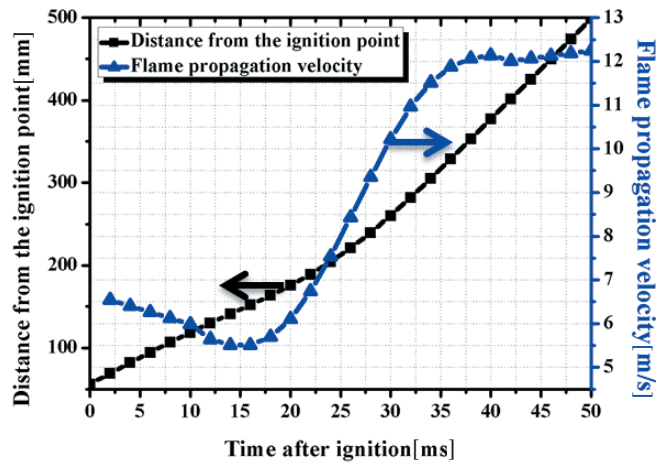
its oxides, the combustion process of a titanium particle could be explained as follows. The solid titanium particle was heated when it approached the combustion zone front. Next, as the titanium particle temperature increased, oxidation reactions occurred on the surface of the titanium particle, forming an oxide coating. The further increase of the temperature resulted in the reaction of the titanium particle in either the liquid phase or the gas phase. Because of the higher temperature of the reaction, an internal stress was formed inside the titanium particles due to the thermal expansion of the liquid or gaseous titanium. When the stress reached a certain threshold, a microexplosion phenomenon occurred in the particle burning process, as shown in Figure 8²⁾.

3.3 Propagation velocities of the combustion zone

The leading edge of the combustion zone was observed to be smooth and clear. The propagation velocity of the combustion zone was measured by examining the movement of its leading edge. Figure 9 shows the relationships between the distance from the ignition point and the propagation velocities of the combustion zone with time after the ignition at two concentrations. The propagation velocities of the combustion zone were not constant. The flames accelerated in the chamber, although there was slight fluctuation. Fluctuation phenomena in dust flame propagation have been observed and discussed in our previous study⁶⁾. The most probable mechanism of this phenomenon was dust stratification as a result of the cooling effect of hot combustion gases by the walls (somewhat analogously to tulip flame formation in a closed vessel). The acceleration of the flame propagation could be attributed to the effect of the thermal expansion of the combustion products. Although the calculated stoichiometric concentration for reaction with air was 419



Concentration- $500 \text{ g}\cdot\text{m}^{-3}$



Concentration- $1000 \text{ g}\cdot\text{m}^{-3}$

Figure 9 Relationships between flame propagation velocity and the flame front position with time at two concentrations.

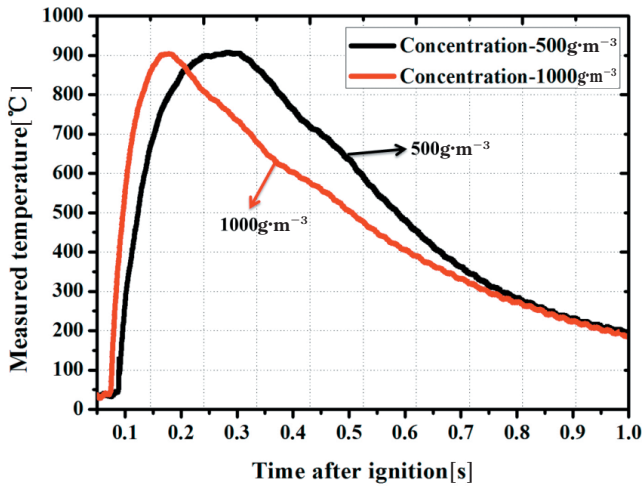


Figure10 Measured temperature profiles of the combustion zone at two concentrations.

$\text{g}\cdot\text{m}^{-3}$, the flame propagation was faster at $1000\text{ g}\cdot\text{m}^{-3}$ than at $500\text{ g}\cdot\text{m}^{-3}$. Similarly, Cashdollar⁵⁾ found that the maximum explosion pressures and rates of pressure increase for the titanium dust occurred at dust concentrations much higher than the stoichiometric value of $419\text{ g}\cdot\text{m}^{-3}$.

3.4 Temperature profile of the combustion zone

A fine thermocouple was used to measure the combustion zone temperature. The measured temperature profiles of the combustion zone at two titanium concentrations are shown in Figure 10. It is clearly observed that the temperature peaked within several tenths of a millisecond and that the combustion reaction was very intensive.

To compensate for the effect of thermal inertia for the thermocouple, the experimental results must be rectified. Assuming that the convective heat transfer to the thermocouple wire predominates over the radiative and conductive contributions, the temperature value measured by the thermocouple can be compensated as follows¹⁸⁾:

$$T = T_m + \tau \frac{dT_m}{dt} \quad (2)$$

Where T_m is the temperature measured by the thermocouple, and τ is the time constant of the thermocouple, which can be written as:

$$\tau = \frac{\rho c_p d^2}{6Nu\lambda_g} \quad (3)$$

Where c_p and ρ are the specific heat and density of the Pt-Pt/Rh13% metal, respectively; d is the diameter of the junction of the thermocouple; λ_g is the thermal conductivity of ambient air; and Nu is the Nusselt number, which can be written as:

$$Nu = 2.0 + 0.60\text{Re}^{1/2} \text{Pr}^{1/3} \quad (4)$$

Re is the Reynolds number, and Pr is the Prandtl number. In our experiments, the value of τ is approximately $6.7 \times 10^{-3}\text{ s}$.

The temperatures corrected by Equation (2) are shown in Figure 11. The position at which the temperature began

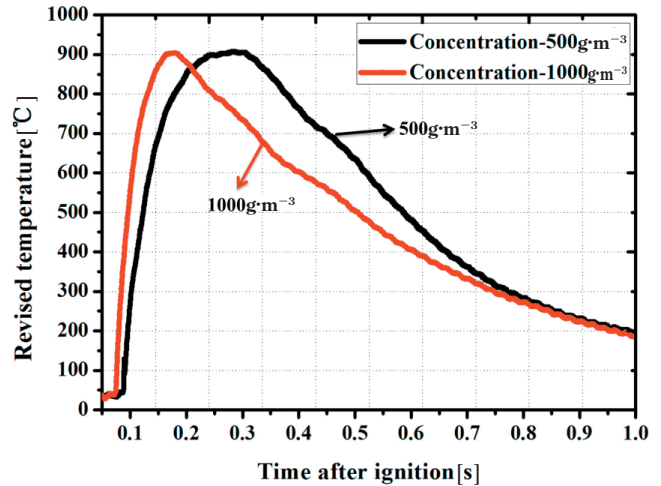


Figure11 Revised temperature profiles of the combustion zone at two concentrations.

to increase indicated the front of the preheated zone. At a titanium concentration of $500\text{ g}\cdot\text{m}^{-3}$, the temperature began to increase at 76 ms, rising quickly and peaking at 1874.38°C at 283 ms. However, at a titanium concentration of $1000\text{ g}\cdot\text{m}^{-3}$, the temperature began to increase at 64 ms and peaked at 1910°C at 163 ms. Both of these temperatures are lower than the calculated adiabatic flame temperature of 3450 K at the stoichiometric concentration but higher than the calculated adiabatic flame temperature of 1420 K at the lean limit. The reason for this discrepancy is that flame propagation is never truly adiabatic, and a variety of complex loss processes occur that inevitably compete with the normal flame propagation processes. Based on the temperature profiles presented above, it can be inferred that the combustion zone was thick, which indicated a longer burning time for these particles.

4. Conclusions

In this study, the flame propagation processes and temperature profiles of titanium particle clouds with two different titanium concentrations in a one end closed chamber were recorded by a high-speed video camera and a fine thermocouple, and the following results were obtained:

- (1) The combustion state of the titanium particles strongly depends on the titanium concentration. At the stoichiometric concentration, a homogeneous mechanism is dominant for titanium particle burning. In contrast, at the lean limit, a heterogeneous surface phase oxidation mechanism may be the only realistic mechanism.
- (2) The flames propagated quickly and emitted strong white light. The length of the luminous zone increased during the flame propagation, and a thin yellow light zone gradually appeared in front of the white light zone. A microexplosion phenomenon usually occurred in the particle burning process.
- (3) The flames accelerated in the chamber, although they fluctuated with time. The most probable mechanism for the fluctuation phenomenon was dust stratification as a result of the cooling effect of hot combustion gases by the

walls. The flame propagation was faster at a dust concentration of $1000 \text{ g}\cdot\text{m}^{-3}$ than at $500 \text{ g}\cdot\text{m}^{-3}$.

(4) The temperature began to increase earlier and reached a higher value at a dust concentration of $1000 \text{ g}\cdot\text{m}^{-3}$ than at a dust concentration of $500 \text{ g}\cdot\text{m}^{-3}$.

References

- 1) E. Shafirovich, S. K. Teoh, and A. Varma, *Combust. Flame*, 152, 262–271(2008).
- 2) S. Kelzenberg, V. Weiser, E. Roth, O. Schulz, and N. Eisenreich, Proc. ECM 2009 Fourth European Combustion Meeting, 1–6, The British Section of the Combustion Institut, Vienna(2009).
- 3) I. E. Molodetsky and E. P. Vicenzi, *Combust. Flame*, 112, 522–532(1998).
- 4) M. Hertzberg, I. A. Zlochower, and K. L. Cashdollar, Proc. 24th Symposium (International) on Combustion, 1827–1835, The Combustion Institute, Pittsburgh(1992).
- 5) K. L. Cashdollar and I. A. Zlochower, *J. Loss Prev. Proc. Ind.*, 20, 337–348(2007).
- 6) W. Gao, R. Dobashi, T. Mogi, J. H. Sun, and X. B. Shen, *J. Loss Prev. Proc. Ind.*, 25, 993–999(2012).
- 7) S. F. Wang, Y. K. Pu, F. Jia, A. Gutkowski, and J. Jarosinski, *Combust. Sci. Technol.*, 178, 1957–1975(2006).
- 8) C. Proust and B. Veyssiere, *Combust. Sci. Technol.*, 62, 149–172(1988).
- 9) O. S. Han, M. Yashima, T. Matsuda, H. Matsui, A. Miyake, and T. Ogawa, *J. Loss Prev. Proc. Ind.*, 14, 153–160(2001).
- 10) O. S. Han, M. Yashima, T. Matsuda, H. Matsui, A. Miyake, and T. Ogawa, *J. Loss Prev. Proc. Ind.*, 13, 449–457(2000).
- 11) R. Dobashi and K. Senda, *J. Loss Prev. Proc. Ind.*, 19, 149–153(2006).
- 12) W. J. Ju, R. Dobashi, and T. Hirano, *J. Loss Prev. Proc. Ind.*, 11, 423–430(1998).
- 13) W. Gao, S. J. Zhong, T. Mogi, H. Y. Liu, J. Z. Rong, and R. Dobashi, *J. Loss Prev. Proc. Ind.*, 26, 186–196(2013).
- 14) National Institute of Standards and Technology, “NIST Chemistry WebBook”, <http://webbook.nist.gov/chemistry/>.
- 15) P. W. Gilles, K. D. Carlson, H. F. Franzen, and P. G. Wahlbeck, *J. Chem. Phys.*, 46, 2461–2465(1967).
- 16) W. O. Groves, M. Hoch, and H. L. Johnston, *J. Phys. Chem.*, 59, 127–131(1955).
- 17) W. Gao, T. Mogi, J. H. Sun, and R. Dobashi, *Fuel*, 113, 86–96(2013).
- 18) A. Ballantyne and J. B. Moss, *Combust. Sci. Technol.*, 17, 63–72(1977).